

## 2.11 Fabrication of cavity structures on GaAs(110)

Embedding quantum well (QW) structures into microcavities enhances the conversion efficiency of photons to electronic excitations, which is of great interest for, e.g., spin polarization experiments. In this case, the spin lifetimes depend sensitively on the orientation of the GaAs substrate. It was shown by transport experiments mediated by surface acoustic waves that GaAs/(Al,Ga)As QWs with (110) orientation exhibit a much longer spin lifetime than QWs with (001) orientation.

Contrary to the well-established GaAs/AlAs cavity structures on GaAs(001), remarkable differences exist for structures with the (110) orientation. The reduced number of active glide systems leads to a pronounced anisotropy of strain relaxation. Furthermore, there are large differences in the elastic behavior between the two orientations and in the relaxation of accumulated elastic strain.

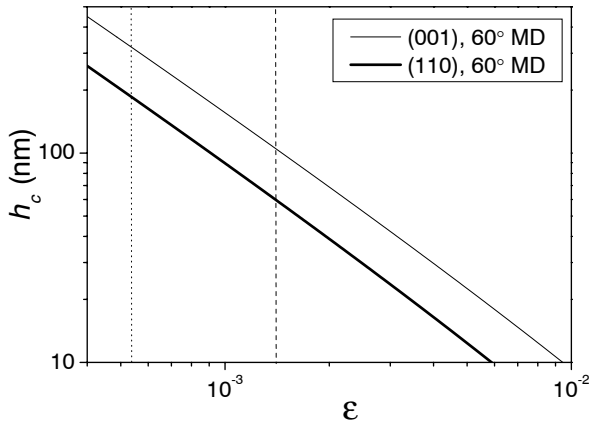


Fig. 30. Critical thickness  $h_c$  as a function of strain  $\varepsilon$  for [001] and [110] growth directions. The dashed line denotes the strain for AlAs on GaAs, the dotted line for a DBR made of an SPSL with  $\bar{x}_{Al} = 0.9$  and an SPSL with  $(\bar{x}_{Al} = 0.1)$  designed for a center wavelength of 850 nm.

$b$ , the strain by  $\varepsilon$ , and  $\theta = 60^\circ$ . The biaxial elastic moduli  $M_{001}$  and  $M_{110}$  have been reported by W. D. Nix *et al.* [Metall. Transact. A **20**, 2217 (1989)]. The relation  $h_c$  vs.  $\varepsilon$  is displayed for films grown on GaAs(001) and (110) substrates in Fig. 30, evidencing that, compared with the (001) orientation, values of  $h_c$  are lower for films with (110) orientation.

Distributed Bragg reflectors (DBR) and cavity structures were grown by molecular-beam epitaxy at a temperature of 490 °C, a beam equivalent pressure ratio of 45 and a growth rate of 500 nm/h on GaAs(110) substrates. The structures were designed for the wavelength range from 810 nm to 980 nm, which allows the use of GaAs-QWs or (In,Ga)As-QWs. The  $\lambda/4$ -layers of the DBR with the higher refractive index, which are realized by short-period superlattices (SPSLs), contain 10% Al.

In Fig. 31, the cross-sectional scanning-electron-microscope (SEM) image of a 10-pair DBR is shown. The DBR is composed of  $\lambda/4$ -thick AlAs layers and  $\lambda/4$ -thick SPSL stacks com-

As an important parameter, the critical thickness  $h_c$  gives an estimated lower limit for the onset of relaxation by 60° misfit dislocations (MD) emerging by means of preexisting threading dislocations. Using the Matthews Blakeslee relation for a single heterostructure, we obtain

$$h_c = \frac{\mu b [1 - \nu \cos^2(\theta)]}{4 \pi (1 - \nu) M_{hkl} \cos(\lambda) \varepsilon} \left[ \ln\left(\frac{h_c}{b}\right) + 1 \right].$$

For (001),  $\lambda = 60^\circ$ , the shear modulus  $\mu = 3.25 \times 10^{10}$  N/m<sup>2</sup>, the Poisson ratio  $\nu = 0.321$ . For (110),  $\lambda = 45^\circ$ ,  $\mu = 4.76 \times 10^{10}$  N/m<sup>2</sup>,  $\nu = 0.224$ . The Burgers vector is denoted by

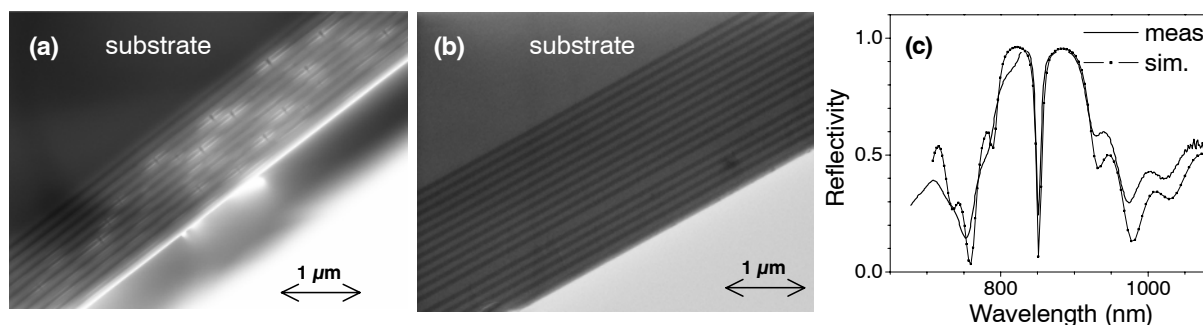


Fig. 31. Cross-sectional scanning electron micrographs of (a) a 10-pair DBR made of AlAs/SPSL ( $\bar{x}_{\text{Al}}=0.1$ ) and (b) a  $\lambda/2$  cavity structure with 10.5/5-pair DBRs made of an SPSL with  $\bar{x}_{\text{Al}} = 0.9$  and an SPSL with  $\bar{x}_{\text{Al}} = 0.1$ . Dark stripes in (a) represent AlAs and in (b) SPSL with  $\bar{x}_{\text{Al}} = 0.9$ . (c) Optical reflectivity spectrum of the  $\lambda/2$  cavity structure shown in (b) together with a simulation using layer thicknesses obtained from x-ray diffraction. The plateau of the measured reflectivity was normalized to the calculated one.

posed of the binary compounds AlAs and GaAs. The image reveals the existence of a larger number of structural defects, which are located in the 72-nm-thick AlAs layer. The nature of these defects is currently under investigation. According to Fig. 30,  $h_c$  for AlAs amounts to about 66 nm. In agreement with the observation, defects emerge between the first and second double layer. For the fabrication of optically efficient QW samples, the generation of these defects connected with strain relaxation has to be prevented. Therefore, in a next step, the 72 nm-thick AlAs layers are also replaced by SPSLs. The DBRs consist of SPSL stacks made of 0.4-nm-thick AlAs films as well as 3.6-nm-thick GaAs films and 3.6-nm-thick AlAs films as well as 0.4-nm-thick GaAs films with an averaged Al mole fraction  $\bar{x}_{\text{Al}} = 0.1$  and 0.9, respectively. DBRs and cavity structures are now free of defects and DBRs with higher stack numbers can be fabricated [cf. Fig. 31(b)]. Under the assumption that the strain is shared between both strained  $\lambda/4$ -SPSLs, the calculated value  $h_c$  amounts to 186 nm (vertical dotted line in Fig. 30) for a DBR stack with (110) orientation as implemented into the cavity structure shown in Fig 31(b). Contrary to the observation, relaxation should also occur. However, the SPSL obviously prevents the motion or the generation of MDs. It is assumed that the insertion of SPSLs improves the smoothness of all interfaces. As a result, there are almost no centers with sufficiently low energetic barriers for the nucleation of MDs.

The optical reflectivity of a defect-free  $\lambda/2$  cavity structure as designed for the center wavelength of 850 nm [cf. Fig. 31(b)] is displayed in Fig. 31(c). The reflectivity is in good agreement with the simulation which is based on layer thicknesses derived from x-ray diffraction. The structural degradation concomitant with strain relaxation, which strongly develops in layer stacks with (110) orientation, is successfully suppressed replacing the thick AlAs layers by SPSL stacks. This approach is promising for the fabrication of high-quality QW cavity structures grown on GaAs(110).

(R. Hey, M. Höricke, U. Jahn)